Research in Astron. Astrophys. **2013** Vol. **13** No. **12**, 1438–1444
*http://www.raa-journal.org* *http://www.iop.org/journals/raa*

*Research in Astronomy and Astrophysics*

# Asteroseismology of DAV white dwarf stars and G29–38

Yan-Hui Chen[1,2,3] and Yan Li[1,2]

[1] Yunnan Astronomical Observatory, Chinese Academy of Sciences, Kunming 650011, China; *yanhuichen1987@ynao.ac.cn, ly@ynao.ac.cn*
[2] Key Laboratory for the Structure and Evolution of Celestial Objects, Chinese Academy of Sciences, Kunming 650011, China
[3] University of Chinese Academy of Sciences, Beijing 100049, China

Received 2013 April 28; accepted 2013 July 24

**Abstract** Asteroseismology is a powerful tool used for detecting the inner structure of stars, which is also widely used to study white dwarfs. We discuss the asteroseismology of DAV stars. The period-to-period fitting method is discussed in detail, including its reliability in detecting the inner structure of DAV stars. If we assume that all observed modes of some DAV stars are the $l = 1$ cases, the errors associated with model fitting will be always large. If we assume that the observed modes are composed of $l = 1$ and 2 modes, the errors associated with model fitting in this case will be small. However, there will be modes identified as $l = 2$ that do not have observed quintuplets. G29–38 has been observed spectroscopically and photometrically for many years. Thompson et al. made $l$ modes identifications in the star through the limb darkening effect. With 11 known $l$ modes, we also study the asteroseismology of G29–38, which reduces the blind $l$ fittings and is a fair choice. Unfortunately, our two best-fitting models are not in line with the previous atmospheric results. Based on factors like only a few observed modes, stability and identification of eigenmodes, identification of spherical degrees, construction of physical and realistic models and so on, detecting the inner structure of DAV stars by asteroseismology needs further development.

**Key words:** stars: oscillations (including pulsations) — stars: individual (G29–38) — white dwarfs

## 1 INTRODUCTION

White dwarfs are the final evolutionary stage of about 98% of stars and some of them are $g$-mode pulsators (Winget & Kepler 2008). Along the cooling curve of white dwarfs, there are DOV (GW Vir), DBV (V777 Her) and DAV (ZZ Ceti) instability strips. DA white dwarfs comprise about 80% of all white dwarfs and DA white dwarf seismology is a focus of research in this field of study (Bischoff-Kim & Metcalfe 2011). Asteroseismology is a powerful tool used to analyze the inner structure of stars. By comparing the calculated results of models in grids, a best-fitting model will be selected which can, in principle, describe the inner structure of the observed star.

Photometric observations taken over a long time that have high signal-to-noise values are required to ensure an effective identification of mode of oscillation can be made. For this work, there

are sometimes combination frequencies, especially at the red edge of the instability strip, where the convection is efficient. Selecting the "real modes" from combination frequencies is an important task, which is related to whether we are fitting eigenmodes. Basically, if there are no parent modes (A and B), the corresponding daughter mode (C = A + B) will be considered as a real mode. However, if there is a relation of A + B = C for the three frequencies, we should decide we should decide which is the linear combination. Each eigenmode is characterized by a group of indices ($k$, $l$, $m$), where $k$ is the radial order, $l$ is the spherical degree and $m$ is the azimuthal order. The radial orders are impossible to determine from observations, which describe the nodes of standing waves inside a star that are radial eigenfunctions. The values of $l$ and $m$ can be constrained by observing rotational splits. Actually, if we observe triplets, the modes will be considered $l = 1$ modes. If we observe quintuplets, the modes will be considered $l = 2$ modes. For stars in the class PG 1159, the quintuplets have been observed and identified, such as PG 1159–035 (Costa et al. 2008). For GD358, quintuplets are also observed (Provencal et al. 2009). However, as far as we know, no quintuplets have been observed for DAV stars, which may be caused by small amplitudes and the variabilities of amplitude and frequency for quintuplet modes. Moreover, the triplets can be observed in DAV stars, such as EC14012–1446 (Handler et al. 2008; Provencal et al. 2012).

Since DAV stars have low luminosity and low effective temperature, it is a challenge to analyze them with methods from asteroseismology as only a few modes can be observed. It is necessary to find a proper method to study the few modes. Winget et al. (1981) first put forward the idea that some modes could be trapped in a hydrogen atmosphere, which are called trapped modes. Trapped modes are effective for studying DAV stars, especially for the hydrogen layer mass. In previous works (e.g. Brassard et al. 1992; Córsico et al. 2002; Benvenuto et al. 2002), trapped modes were identified by selecting the minimal spacing of a period on a plot of the spacing for period versus consecutive period. Such a method requires a series of pulsation periods to be continuously observed in $k$, and missing a few modes breaks the line for period into several segments, which makes it difficult to definitively recognize the trapped modes. According to the asymptotic theory, g-modes with large radial orders approximately follow an equal spacing law in terms of their pulsation periods. Córsico et al. (2007) took the deviations from a uniform period spacing to study the PG 1159-type star PG0122+200. Bradley & Winget (1994) also applied this method to investigate the properties of trapped modes for GD358 and Handler et al. (2002) applied it to the analysis of the DBV star CBS114. The deviations from regular spacing for the mean period are independent of the continuity in $k$ and only depend on the relative identification of $k$. Occasionally missing one or two modes does not affect the deviations of other modes. However, this method depends on an accurate identification of $l$ and the identification of the relative value of $k$.

Trapped modes can be studied on the diagram of spacing for period versus consecutive period, and can also be studied by deviating from the mean period spacing. For asteroseismology, the fittings to observed periods with calculated periods in grid models, namely detailed period-to-period fittings, are commonly used. Fu et al. (2013) performed an asteroseismology study for HS 0507+0434B, including the calculations of the model with a grid (Dolez & Vauclair 1981) and detailed period-to-period fittings. Castanheira & Kepler (2009) did the asteroseismology study for 83 ZZ Ceti stars by using detailed period-to-period fittings. The grid models were generated by the White Dwarf Evolution Code (WDEC) (Castanheira & Kepler 2008). Also, with LPCODE, Romero et al. (2012) made fully evolutionary white dwarf models, taking into account element diffusion. They also studied asteroseismology of DAV stars by performing detailed period-to-period fittings. In this paper, we are interested in the detailed period-to-period fitting method. If there is little or no rotational splitting that can be observed, we usually assume there are modes $l = 1$, according to the equal spacing law, or a mixture of $l = 1$ and $l = 2$ modes. However, these are only assumptions. Thompson et al. (2008) identified the spherical degree for G29–38 through the limb darkening effect. With their known $l$ modes, we investigate asteroseismology for G29–38 by fittings of the model with a grid in this paper. Then, we discuss the reliability of asteroseismology work for DAV stars.

## 2 THE PREVIOUS STUDIES OF G29–38

G29–38 has an extensive range of both spectroscopic and photometric observations. For example, with optical spectrophotometry, Bergeron et al. (1995) calculated the atmospheric parameters ($T_{\rm eff}$ = 11 820 K and $\log g = 8.14$), adopting ML2/$\alpha = 0.6$. By fitting Balmer lines H$\beta$ to H8, Koester et al. (1997) obtained $T_{\rm eff}$ = 11 600 K and $\log g = 8.05$. Clemens et al. (2000) also fitted lines H$\beta$ to H11 in a time-averaged spectrum and gave their best-fitting model with $T_{\rm eff}$ = 11 850 K and $\log g = 8.05$. Koester et al. (2005) studied the Ca abundance and gave the atmospheric parameters for G29–38 (WD 2326+049) of $T_{\rm eff}$ = 12 100 K and $\log g = 7.9$. In 2009, Koester et al. studied high-resolution UVES/VLT spectra and reported the new atmospheric parameters of $T_{\rm eff} = 11\,485 \pm 8$ K and $\log g = 8.007 \pm 0.002$ (Koester et al. 2009).

Kleinman et al. (1998) compiled a summary of over 1100 hours of time-series photometry including two WET runs, a double-site venture between SAAO and McDonald Observatory, and many years of single site observations. They obtained data in 1985 and from 1988 to 1994. Some modes were observed in some years but disappeared in other years. This phenomenon is common in other DAV stars, such as EC14012–1446 (Handler et al. 2008; Provencal et al. 2012). The stability of the eigenmode is another research topic. Assuming the eigenmodes to be the $l = 1$ modes, Kleinman et al. (1998) proposed a method to identify radial orders. Because all the modes were assumed to be $l = 1$, the model fittings did not have a very good result. As described by Kleinman et al. (1998), the critical mismatch of the $l = 1$ modes were $k$ = 1 and $k$ = 2 cases.

Their identified eigenmodes are shown in the first column in Table 1. Moreover, the second column expresses the mean values of the modes from different observations from 1985 to 1993, which are chosen by Castanheira & Kepler (2009). Assuming they are $l = 1$ modes, Castanheira & Kepler (2009) obtained their best-fitting model ($T_{\rm eff} = 11\,700$ K, $M_* = 0.665\,M_\odot$, $M_{\rm He} = 10^{-2}\,M_*$ and $M_{\rm H} = 10^{-8}\,M_*$). Moreover, assuming they are $l = 1, 2$ modes, Romero et al. (2012) showed that their best-fitting model had the parameters $T_{\rm eff} = 11\,471 \pm 60$ K, $M_* = 0.593 \pm 0.012\,M_\odot$, $M_{\rm He} = 2.39 \times 10^{-2}\,M_*$, $M_{\rm H} = (4.67 \pm 2.83) \times 10^{-10}\,M_*$ and $\log g = 8.01 \pm 0.03$.

**Table 1** Detected modes for G29–38

| $P^{\rm obs1}$ | $P^{\rm obs2}$ | $P^{\rm obs3}(l)$ |
|---|---|---|
| 110 | – | – |
| 177 | – | – |
| 237 | 218.7 | – |
| 284 | 283.9 | 284(1) |
| 355 | 363.5 | 353(4or3) |
| 400 | 400.5 | – |
| | – | 431(1) |
| 500 | 496.2 | – |
| 552 | – | – |
| 610 | 614.4 | 614(1) |
| 649 | 655.1 | 655(1) |
| 678 | – | 681(2) |
| 730 | – | – |
| 771 | 770.8 | 776(2) |
| 809 | 809.4 | 815(1) |
| | – | 835(1) |
| 860 | 859.6 | – |
| 894 | 894.0 | – |
| 915 | – | 920(2) |
| | – | 937(1) |
| | 1150.5 | – |
| 1147 | – | – |
| | 1185.6 | – |
| 1240 | 1239.9 | – |

The asteroseismology results are consistent with atmospheric parameters from Koester et al. (2009). However, for the 14 modes, their results show 13 $l = 2$ modes and only one $l = 1$ mode. This makes us wonder whether there are really so many $l = 2$ modes that were observed.

Robinson et al. (1995) firstly introduced a method to determine $l$ by studying the limb darkening effect. The use of time series at various wavelengths, including UV, allows us to use the different wavelength response of the different $l$ degrees to the limb darkening, due to the different geometry of the different $l$ values, which can help in identifying $l$. With this method, Thompson et al. (2008) made $l$ identifications for G29–38. Their results are shown in the third column of Table 1, which include contributions from Clemens et al. (2000) and Kotak et al. (2002). The identifications of $l$ are shown in the parenthesis. With spherical degrees being identified, we can again study asteroseismology of G29–38.

## 3 MODEL CALCULATIONS AND FITTING RESULTS

Our white dwarf models are generated by the WDEC, which was first written by Schwarzschild and then modified by Kutter & Savedoff (1969), Lamb & van Horn (1975) and Wood (1990). Itoh et al. (1983) introduced radiative opacities and conductive opacities to the algorithm. The equation of state (eos) is composed of two parts. In the degenerate and ionized core, it takes the eos of Lamb (1974), but in the outer layer, it adopts the eos of Saumon et al. (1995). For special C/O mixtures and H/He mixtures, the technique of additive volume is adopted (Fontaine et al. 1977). For element diffusion, the effect of gravity sedimentation results in a composition that shows a stratified structure. However, the chemical gradient mixes elements in transition regions. DAV stars have experienced evolutionary changes over a long time and their shell profile is likely to be in or close to equilibrium. So, WDEC adopts equilibrium profiles proposed by Wood (1990) as an approximation of H/He and He/C mixtures. Convective mixing should not reach the H/He transition zone in the temperature range of the ZZ Ceti instability strip except in the extremely low mass of the hydrogen layer. Adopting the mixing length theory of Böhm & Cassinelli, the mixing length parameter ($\alpha$) is defined as a ratio of mixing length to pressure scale height (Bohm & Cassinelli 1971; Tassoul et al. 1990). All of the models are results of evolutionary calculations. The initial effective temperature is about 100 000 K and the total number of mesh grids is about 1000. With these models, we numerically solve the full equations of linear and adiabatic oscillation, which successively calculate eigenfrequencies through scanning.

Then, we briefly present the grid models we adopt. Four quantities ($T_{\rm eff}$, $M_*$, $M_{\rm H}$ and $M_{\rm He}$) are involved in the network. The effective temperature ($T_{\rm eff}$) varies from 11 000 K to 12 000 K with a step of 50 K. The total stellar mass ($M_*$) changes from $0.600\,M_\odot$ to $0.800\,M_\odot$ with a step of $0.005\,M_\odot$. $\log(M_{\rm H}/M_*)$ varies from $-10$ to $-4$ with a step of 0.5. Also, $\log(M_{\rm He}/M_*)$ only equals $-4, -3.5, -3, -2.5$ and $-2$. The mixing length parameter ($\alpha$) equals 0.6, the same as Bergeron et al. (1995). For a profile of the core composition, Castanheira & Kepler (2008) adopted the homogeneous profile. In order to be closer to the composition profile shown in Romero et al. (2012), we take 20% carbon in the center of the stellar C/O core, 60% carbon on the surface of the C/O core and a linear profile between the two ends. Then, the grid models are calculated.

In order to select the best-fitting model, we introduce the commonly used variable,

$$\begin{aligned}\phi &= \phi(M_*, \log(M_{\rm H}/M_*), \log(M_{\rm He}/M_*), T_{\rm eff}) \\ &= \frac{1}{n}\sum(|P^{\rm th}(l) - P^{\rm obs}(l)|)\,. \end{aligned} \quad (1)$$

In the above equation, $n$ is the number of observed periods we adopt. $P^{\rm th}(l)$ is the model periods calculated and $P^{\rm obs}(l)$ is the real periods observed. It is worth mentioning that the absolute difference is expressed in terms of the same spherical degree. The model with the smallest $\phi$ is considered to be the best-fitting one.

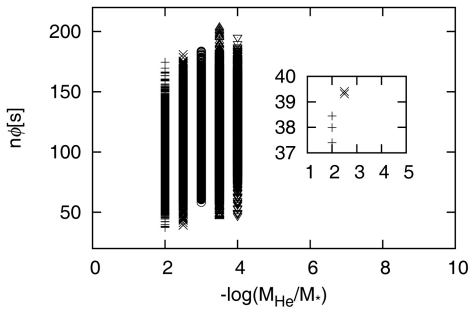


**Fig. 1** Diagram for selecting the best-fitting models. Being from Equation (1), the ordinate is $n\phi$ and the abscissa is the helium layer mass ($-\log(M_{\rm He}/M_*)$). The diagram shows values of $n\phi$ for all of the grid models and there is a magnified subgraph.

**Table 2** Our Model Results for G29–38

| $P^{\rm obs}(l)$ | $P^{\rm mod1}(l)$ | $\Delta P(1)$ | $\phi(1)$ | $P^{\rm mod2}(l)$ | $\Delta P(2)$ | $\phi(2)$ |
|---|---|---|---|---|---|---|
| 284(1) | 285.75(1) | 1.75 | 3.40 | 279.04(1) | 4.96 | 3.58 |
| 353(4/3) | 353.38(3) | 0.38 | | 357.52(3) | 4.52 | |
| 431(1) | 429.55(1) | 1.45 | | 433.98(1) | 2.98 | |
| 614(1) | 606.73(1) | 7.27 | | 609.12(1) | 4.88 | |
| 655(1) | 644.80(1) | 10.20 | | 658.11(1) | 3.11 | |
| 681(2) | 683.74(2) | 2.74 | | 680.69(2) | 0.31 | |
| 776(2) | 776.54(2) | 0.54 | | 777.18(2) | 1.18 | |
| 815(1) | 810.55(1) | 4.45 | | 815.29(1) | 0.29 | |
| 835(1) | 838.16(1) | 3.16 | | 847.65(1) | 12.65 | |
| 920(2) | 917.64(2) | 2.36 | | 918.17(2) | 1.83 | |
| 937(1) | 940.09(1) | 3.09 | | 934.38(1) | 2.62 | |

After all the grid-models are fitted to the identified spherical degree modes, the fitting results are obtained and shown in Figure 1. Being from Equation (1), the ordinate is $n\phi$ and the abscissa is the helium layer mass ($-\log(M_{\rm He}/M_*)$). At each helium branch, there are grid models of different total stellar masses, different effective temperatures and different hydrogen layer masses. In addition, there is a magnified subgraph. Therefore, we can clearly see that the minimal values of $n\phi$ are located in the branches of $\log(M_{\rm He}/M_*) = -2$ and $-2.5$. For $\log(M_{\rm He}/M_*) = -2$, we take the three best-fitting models of $n\phi$ = 37.40, 37.99 and 38.45. They have the same helium layer mass and hydrogen layer mass, and close effective temperatures and total stellar masses ((11 900 K, 0.790 $M_\odot$), (11 750 K, 0.795 $M_\odot$) and (11 850 K, 0.790 $M_\odot$)). We choose the model of $n\phi$ = 37.40 as model1. For $\log(M_{\rm He}/M_*) = -2.5$, we take the two best-fitting models of $n\phi$ = 39.32 and 39.41. They have the same helium layer mass and hydrogen layer mass, and close effective temperatures and total stellar masses ((11 250 K, 0.780 $M_\odot$) and (11 150 K, 0.785 $M_\odot$)). We choose the model of $n\phi$ = 39.32 as model2. The results of model1 and model2 are shown in Table 2.

For model1, $T_{\rm eff} = 11\,900$ K, $M_* = 0.790\ M_\odot$, $M_{\rm He} = 10^{-2}\ M_*$, $M_{\rm H} = 10^{-4}\ M_*$, $\log(g) = 8.30$ and $\phi = 3.40$, while, for model2, $T_{\rm eff} = 11\,250$ K, $M_* = 0.780\ M_\odot$, $M_{\rm He} = 3.16 \times 10^{-3}\ M_*$, $M_{\rm H} = 3.16 \times 10^{-6}\ M_*$, $\log(g) = 8.30$ and $\phi = 3.58$. Though 3.40 is less than 3.58, they are basically in the same level. We cannot decide which one is better. What puzzles us is that the fitting error is a little large for the mode of 655 s in our model1 with 644.80 s, for the mode of 835 s in our model2 with 847.65 s and for the mode of 655.1 s in the model of Romero et al. (2012) with 644.728 s. There is always a relatively large error for at least one mode in each model. For the two models, the gravitational acceleration is larger than the atmospheric results. Anyway, it is a fair

choice to fit the known $l$ modes and fitting the known $l$ modes can reduce the blind $l$ fittings. If we do not know the spherical degree of each mode, we can just assume $l = 1$ or $l = 1, 2$.

## 4 DISCUSSION AND CONCLUSIONS

In this paper, we focus on the detailed period-to-period fitting method used in asteroseismology. If we assume that all observed eigenmodes are $l = 1$ modes, the fitting error will be large. For example, $\phi$ is 7.47 and 7.01 for the two best-fitting models respectively for EC14012–1446 in the work of Castanheira & Kepler (2009). Assuming the same nine observed periods as $l = 1, 2$ modes, $\phi$ is 2.54 in the work of Romero et al. (2012) for EC14012–1446. The mean period spacing for different spherical degrees is,

$$\Delta\bar{\mathrm{P}}(l) = \frac{2\pi^2}{\sqrt{l(l+1)}\int_0^R \frac{N}{r} dr} \,. \tag{2}$$

In the above equation, $N$ is buoyancy frequency. According to the equation, the larger the spherical degree, the smaller the mean period spacing. To some extent, if we enlarge the spherical degree, the mean spacing between periods will decrease and the fitting error will also decrease. For G29–38, assuming $l = 1, 2$, $\phi$ is 2.84 in the work of Romero et al. (2012). The effective temperature and gravitational acceleration are consistent with the atmospheric results of Koester et al. (2009). Their white dwarf models are fully evolutionary and take the element diffusion into account. At least these models are more realistic for the profile of the core composition, which is really from element burning. However, in their fittings, the 14 observed modes are 13 $l = 2$ modes and only one $l = 1$ mode. Because there are so many $l = 2$ modes, we think that it is necessary to study asteroseismology of the star with the modes identified in terms of spherical degrees. Thompson et al. (2008) made the $l$ identifications for G29–38 by using the limb darkening effect. With the spherical degree modes being known, we also investigate asteroseismology of G29–38 and the results are different from previous works. The large gravitational acceleration and mass of the thick hydrogen layer are obtained. The result, being different from the previous works that use asteroseismology, is acceptable, because the identification of the spherical degree is at least not the same. Actually, the molecular weight gradient for the core composition profile (20% carbon at the center of the stellar C/O core, 60% carbon on the surface of the C/O core and a linear profile between the two ends) of our models is smaller than the element burning result of Romero et al. (2012). According to the definition of the buoyancy frequency, the square of buoyancy frequency is proportional to the molecular weight gradient multiplied by the square of gravitational acceleration. In order to obtain the same buoyancy frequency, if we take the core composition profile of the element burning result (large molecular weight gradient), the gravitational acceleration will be reduced. This may explain why our gravitational acceleration is greater than the atmospheric results.

Temporarily, we do not consider the errors in models themselves. For the identified eigenmodes, such as in Table 1, there are three columns of periods. Some modes appear in one column but not others. There are also modes like 610, 614.4, 355, 363.5 s and so on. All of these will introduce uncertainties into the model fittings. This phenomenon does not occur in single manifestations. For EC14012–1446, there are nine eigenmodes in Castanheira & Kepler (2009) and 14 eigenmodes ($l = 1$) in Provencal et al. (2012). As we have done here, it seems that taking the known spherical degree modes and doing work in asteroseismology are good choices. At least this approach can reduce the error from blind $l$ fittings, though there are only 11 modes for G29–38 in the third column in Table 1. For DAV stars, asteroseismology depends on at least the following four factors.

(1) In this situation there are only a few modes being observed. The more observed modes there are, the more helpful the model fittings will become.
(2) The complicating factor is stability and identification of eigenmodes. This problem is determining whether we are fitting eigenmodes.

(3) The identification of spherical degrees is also a complicating factor. Blind spherical degree fittings of modes may lead to some erroneous results.
(4) The construction of physical and realistic white dwarf models is related. It is related to whether the models themselves are realistic enough to be used for the asteroseismology of white dwarfs.

**Acknowledgements** This work is supported by the Knowledge Innovation Key Program of the Chinese Academy of Sciences under Grant No. KJCX2-YW-T24 and the Yunnan Natural Science Foundation (Y1YJ011001). We are very grateful to X. J. Lai, Q. S. Zhang, T. Wu and J. Su for their kind discussion and suggestions.

## References

Benvenuto, O. G., Córsico, A. H., Althaus, L. G., & Serenelli, A. M. 2002, MNRAS, 335, 480
Bergeron, P., Wesemael, F., Lamontagne, R., et al. 1995, ApJ, 449, 258
Bischoff-Kim, A., & Metcalfe, T. S. 2011, MNRAS, 414, 404
Bohm, K. H., & Cassinelli, J. 1971, A&A, 12, 21
Bradley, P. A., & Winget, D. E. 1994, ApJ, 430, 850
Brassard, P., Fontaine, G., Wesemael, F., & Hansen, C. J. 1992, ApJS, 80, 369
Castanheira, B. G., & Kepler, S. O. 2008, MNRAS, 385, 430
Castanheira, B. G., & Kepler, S. O. 2009, MNRAS, 396, 1709
Clemens, J. C., van Kerkwijk, M. H., & Wu, Y. 2000, MNRAS, 314, 220
Córsico, A. H., Althaus, L. G., Benvenuto, O. G., & Serenelli, A. M. 2002, A&A, 387, 531
Córsico, A. H., Miller Bertolami, M. M., Althaus, L. G., Vauclair, G., & Werner, K. 2007, A&A, 475, 619
Costa, J. E. S., Kepler, S. O., Winget, D. E., et al. 2008, A&A, 477, 627
Dolez, N., & Vauclair, G. 1981, A&A, 102, 375
Fontaine, G., Graboske, H. C., Jr., & van Horn, H. M. 1977, ApJS, 35, 293
Fu, J.-N., Dolez, N., Vauclair, G., et al. 2013, MNRAS, 429, 1585
Handler, G., Metcalfe, T. S., & Wood, M. A. 2002, MNRAS, 335, 698
Handler, G., Romero-Colmenero, E., Provencal, J. L., et al. 2008, MNRAS, 388, 1444
Itoh, N., Mitake, S., Iyetomi, H., & Ichimaru, S. 1983, ApJ, 273, 774
Kleinman, S. J., Nather, R. E., Winget, D. E., et al. 1998, ApJ, 495, 424
Koester, D., Provencal, J., & Shipman, H. L. 1997, A&A, 320, L57
Koester, D., Rollenhagen, K., Napiwotzki, R., et al. 2005, A&A, 432, 1025
Koester, D., Voss, B., Napiwotzki, R., et al. 2009, A&A, 505, 441
Kotak, R., van Kerkwijk, M. H., & Clemens, J. C. 2002, A&A, 388, 219
Kutter, G. S., & Savedoff, M. P. 1969, ApJ, 156, 1021
Lamb, D. Q., Jr. 1974, Evolution of Pure Carbon-12 White Dwarfs., Ph.D. Thesis, The University of Rochester
Lamb, D. Q., & van Horn, H. M. 1975, ApJ, 200, 306
Provencal, J. L., Montgomery, M. H., Kanaan, A., et al. 2009, ApJ, 693, 564
Provencal, J. L., Montgomery, M. H., Kanaan, A., et al. 2012, ApJ, 751, 91
Robinson, E. L., Mailloux, T. M., Zhang, E., et al. 1995, ApJ, 438, 908
Romero, A. D., Córsico, A. H., Althaus, L. G., et al. 2012, MNRAS, 420, 1462
Saumon, D., Chabrier, G., & van Horn, H. M. 1995, ApJS, 99, 713
Tassoul, M., Fontaine, G., & Winget, D. E. 1990, ApJS, 72, 335
Thompson, S. E., van Kerkwijk, M. H., & Clemens, J. C. 2008, MNRAS, 389, 93
Winget, D. E., & Kepler, S. O. 2008, ARA&A, 46, 157
Winget, D. E., van Horn, H. M., & Hansen, C. J. 1981, ApJ, 245, L33
Wood, M. A. 1990, Astero-archaeology: Reading the Galactic History Recorded in the White Dwarf Stars, Ph.D. Thesis, Texas Univ., Austin